Optica Applicata, Vol. XXXI, No. 1, 2001

Thermal conductivity and temperature distribution in RF excited CO_2, CO, and Xe laser media

EDWARD F. PLIŃSKI, JERZY S. WITKOWSKI

Institute of Telecommunications and Acoustics, Wrocław University of Technology, Wybrzeże Wyspiańskiego 27, 50–370 Wrocław, Poland.

Different methods of calculations of thermal conductivity of gas laser mixtures versus temperature are compared in the paper. Approximation functions describing the experimental data of thermal conductivity and viscosity of chosen gases (CO_2, N_2, He, Xe, CO, O_2 Ar) are given. The formulas introduced and data obtained allow us to predict thermal conductivity and temperature distribution of a typical high power laser gas mixture. Examples of temperature distribution in RF excited CO_2, CO, and Xe laser media are shown. Knowledge of the temperature distribution in the laser cavity can be useful for predicting general optical properties of the laser.

1. Introduction

Designing the gas laser devices requires knowledge about parameters of the laser medium, like gain coefficient (to design properly the optical resonator), operation pressure, properties of the laser plasma (to design the power supply and excitation method), or thermal properties of the medium (to design efficient cooling), *etc.* The temperature of laser mixture can influence optical properties of the laser such as quality of the output beam and its spectral characteristics.

This paper concentrates on thermal properties of the most popular gas laser media in modern RF excited slab-waveguide structures. Three laser media have been chosen for the investigation. These are CO_2, CO, and Xe media. The advantage of such a choice lies in ease of comparing all chosen media in the same laser mechanical structure. Practically, the same RF slab-waveguide can be used for all chosen media by simple exchanging of the gas mixture (and mirrors).

Thermal conductivity of the laser gas mixture determines the temperature of the medium at a given level of the input power. Calculation of the thermal conductivity of gas mixtures requires data for pure components of the mixture. These are thermal conductivity and viscosity of each component. Their experimental values are usually collected and published in tables [1]–[4]. To make them convenient for use empirical equations are derived for futher computerised calculations [5], [6]. These empirical functions are in error with experimental data at high values of temperature. The goal of this paper is to give approximation functions describing the experimental data of thermal conductivity and viscosity of chosen gases for the temperature ranging from 280 to 1500 K. Collected in tables the factors of approximations

functions allow the user to specifity the desired accuracy of calculations. Examples of the thermal conductivity versus temperature are given and compared for typical CO_2, CO and Xe laser gas media. Temperature distributions for the afore mentioned three RF excited laser media in the same structure of the-waveguide are given as well.

Knowledge of the temperature distribution in the laser cavity can be used for predicting general optical properties of the laser.

2. Thermal conductivity of the gas mixtures

The formula for the first approximation to the thermal conductivity $[\lambda_{mix}]_1$ for a multicomponent gas mixture was given by HIRSCHFELDER *et al.* [7, Eq. (8.2–42)]

$$[\lambda_{mix}]_1 = [\lambda_{mix}]_1 - \frac{1}{2} R \sum_{i=1}^{n} \sum_{\substack{j=1 \\ j \neq i}}^{n} \frac{RTx_i x_j}{p[\mathscr{D}_{ij}]_1} \left[\frac{[D_i^T]_1}{x_i M_i} - \frac{[D_j^T]_1}{x_j M_j} \right]^2 \tag{1}$$

where: R – universal gas constant,
T – temperature,
x_i – the molecule fraction of the i-th component,
p – presure,
M_i – molar mass of the i-th component,
$[\mathscr{D}_{ij}]_1$ – the first approximation to the binary diffusion constant,
$[D_i^T]_1$ – the first approximation to the multicomponent thermal diffusion coefficient,

and $[\lambda'_{mix}]_1$ is given by [7, Eq. (8.2–43)]

$$[\lambda'_{mix}]_1 = 4 \begin{vmatrix} L_{11}^{00} & \cdots & L_{1n}^{00} & L_{11}^{01} & \cdots & L_{1n}^{01} & 0 \\ \vdots & \ddots & \vdots & \vdots & \ddots & \vdots & \vdots \\ L_{n1}^{00} & \cdots & L_{nn}^{00} & L_{n1}^{01} & \cdots & L_{nn}^{01} & 0 \\ L_{11}^{01} & \cdots & L_{1n}^{01} & L_{11}^{11} & \cdots & L_{1n}^{11} & x_1 \\ \vdots & \ddots & \vdots & \vdots & \ddots & \vdots & \vdots \\ L_{n1}^{01} & \cdots & L_{nn}^{01} & L_{n1}^{11} & \cdots & L_{nn}^{11} & x_n \\ 0 & \cdots & 0 & x_1 & \cdots & x_n & 0 \end{vmatrix} \Bigg/ \begin{vmatrix} L_{11}^{00} & \cdots & L_{1n}^{00} & L_{11}^{01} & \cdots & L_{1n}^{01} \\ \vdots & \ddots & \vdots & \vdots & \ddots & \vdots \\ L_{n1}^{00} & \cdots & L_{nn}^{00} & L_{n1}^{01} & \cdots & L_{nn}^{01} \\ L_{11}^{01} & \cdots & L_{1n}^{01} & L_{11}^{11} & \cdots & L_{1n}^{11} \\ \vdots & \ddots & \vdots & \vdots & \ddots & \vdots \\ L_{n1}^{01} & \cdots & L_{nn}^{01} & L_{n1}^{11} & \cdots & L_{nn}^{11} \end{vmatrix} \tag{2}$$

where L_{nn}^{ii} – the components given in [7].

After simplifications given by Mason *et al.* the formula for the coefficient of thermal conductivity can be expressed as follows [8]:

$$[\lambda_{mix}]_1 = 4 \begin{vmatrix} L_{11} & \cdots & L_{1n} & x_1 \\ \vdots & \ddots & \vdots & \vdots \\ L_{n1} & \cdots & L_{nn} & x_n \\ x_1 & \cdots & x_n & 0 \end{vmatrix} \Bigg/ \begin{vmatrix} L_{11} & \cdots & L_{1n} \\ \vdots & \ddots & \vdots \\ L_{n1} & \cdots & L_{nn} \end{vmatrix} \tag{3}$$

where L_{ii} and L_{ij} are given by:

$$L_{ii} = -\frac{4x_i^2}{[\lambda_i]_1} - \frac{16T}{25p} \sum_{\substack{k=1 \\ k \neq i}}^{n} \frac{x_i x_k [(15/2) M_i^2 + 4 M_i M_k A_{ik}^*]}{(M_i + M_k)^2 [D_{ik}]_1}, \tag{4}$$

$$L_{ij}(i \neq j) = \frac{16 T x_i x_j M_i M_j (10 - 4A_{ij}^*)}{(M_i + M_j)^2 [D_{ij}]_1} \tag{5}$$

where: $[\lambda_i]_1$ – the first approximation to the thermal conductivity of pure polyatomic component i,

A_{ik}^* – dimensionless ratios of collision integrals [7].

According to MASON *et al.* [8], the off-diagonal elements L_{ij} are much smaller than the diagonal elements L_{ij}, and Eq. (3) can be expanded as follows [7]:

$$\lambda_{mix} = -4 \sum_{i=1}^{n} \frac{x_i^2}{L_{ii}} + 4 \sum_{i=1}^{n} \sum_{\substack{i=1 \\ j \neq i}}^{n} \frac{x_i x_j L_{ij}}{L_{ii} L_{jj}} + \dots . \tag{6}$$

Neglecting the higher summations, it takes the form

$$\lambda_{mix} = \sum_{i=1}^{n} \lambda_i \left[1 + \sum_{\substack{k=1 \\ k \neq i}}^{n} G_{ik} \frac{x_k}{x_i} \right]^{-1} \tag{7}$$

where G_{ik} after some simplifications given by Mason *et al.* takes the form [8]

$$G_{ik} = \frac{1.065}{2\sqrt{2}} \left(1 + \frac{M_i}{M_k} \right)^{-1/2} \left[1 + \left(\frac{\eta_i M_k}{\eta_k M_i} \right)^{1/2} \left(\frac{M_i}{M_k} \right)^{1/4} \right]^2 \tag{8}$$

where: $\eta_{i,k}$ – viscosity of pure components.

3. Thermal conductivity and viscosity of pure components

As seen from Equations (7) and (8), for calculation of the thermal conductivity of any mixture, the thermal conductivity λ_i and viscosity η_i are necessary. These parameters can be obtained in different ways. There are a number of theoretical and empirical formulas describing the thermal conductivity and viscosity of gases. Experimental data are available as well. In the following Sections (3.1 and 3.2) λ_i and η_i obtained theoretically and experimentally are compared in the temperature range of 280 – 1500 K.

3.1. Theoretical analysis

Thermal conductivity was investigated widely by many authors, and practical formula was given by HIRSCHFELDER *et al.* [7, eq. (8.2–31, 33)]

$$[\lambda_i]_1 = \frac{25}{32} C_v \sqrt{\frac{kN_A}{\pi}} \frac{\sqrt{T/M_i}}{\sigma_i^2 \Omega^{(2,2)*}(T_i^*)} \; Eu = 2.6317 \cdot 10^{-23} \times$$

$$\times \frac{\sqrt{T/M_i}}{\sigma_i^2 \Omega^{(2,2)*}(T_i^*)} Eu = [\lambda_i^0]_1 Eu \tag{9}$$

where: λ_i^0 – thermal conductivity that would be obtained if all intgernal degrees of freedom of molecules were "frozen", λ_i – thermal conductivity [W/m·K], T – temperature [K], $T_i^* = kT/\varepsilon_i$ – reduced temperature, M_i – molecular weight of the i-th component [kg/mol], σ_i – collision diameter (characteristic dimension) for specified i-th components [m], ε_i/k – characreristic temperature for specified i-th components, C_v – specific heat = $3k/2$ [J/mol K], k – Boltzmann's constant [J/K], N_A – Avogadro's number [1/mol], $\Omega_{ik}^{(2,2)*}$ – collision integrals for viscosity, Eu – Eucken factor [7].

The Eucken factor is different from unity for polyatomic gases. In this case, appreciable amount of energy is transported by the internal degree fo freedom. The Eucken factor was rigorously derived by HIRSCHFELDER *et al.* and can be expressed as [7]

$$Eu_i = \frac{3}{5} + \frac{4}{15}\left(1 + \frac{C_{pi}}{R}\right) \tag{10}$$

or [8]:

$$Eu_i = 0.115 + 0.354 \cdot \frac{C_{pi}}{R} \tag{11}$$

where: C_{pi} – the constant-pressure molar specific heat capacity of the i-th component (for the monoatomic gases $Eu_i = 1$), R – gas constant.

The constant-pressure molar heat capacity depends on the temperature and can be expressed as [9]

$$C_{pi} = a_i + b_i T + c_i T^2 + d_i T^3 \tag{12}$$

where factors a_i, b_i, c_i and d_i can be found in [9] for the temperature range of 273–1800 K.

The values of T^* vs. $\Omega^{(2,2)*}$ for Lennard–Jones ((6)–(12)) potential are tabulated in [7, Tab. I-M]. They can be approximated with the function [6]

$$\Omega^{(2,2)}(T^*) = 1.16145 T^{*-0.14874} + \frac{0.52487}{\exp(0.7732 T^*)} + \frac{2.16178}{\exp(2.43787 T^*)} - 6.435 \cdot 10^{-4} T^{*0.14874} \sin(18.0323 T^{*-0.7683} - 7.27371). \tag{13}$$

Values of the parameters σ_i and ε_i/k necessary for calculations of thermal conductivity of components of the most popular laser gas mixtures are given in Tab. 1.

It has been proved (Fig. 1, example for CO_2) that calculated values of λ_i in the range from 280 to 1500 K are closer to the experimental data for the Eucken factor taken from Eq. (11) and parameters σ_i and ε_i/k bold-faced in Tab. 1.

Table 1. Force constace σ_i and ε_i/k for Lennard–Jones (6–12) potential for chosen gases [7 — Tab. I-A, p. 1111], [5 — Appendix B]. Eu_1, Eu_2 — Eucken factors according to Eqs. (10) and (11), respectively. Indexes (A), (B), (C), and (a), (b), (c) are explained in Fig. 1.

Gas	ε_i/k [K]	σ_i [Å]	Ref.	Eu_1	Eu_2
CO_2	190.0	3.996	[7]	(a)	(A)
	213.0	**3.987**	[7]	(b)	(B)
	195.2	3.941	[5]	(c)	(C)
Na	91.5	3.681		[7]	
	79.8	3.749		[7]	
	71.4	**3.798**		[5]	
He	10.22	2.576		[7]	
	10.22	**2.551**		[5]	
Xe	229	4.055		[7]	
	231	**4.047**		[5]	
CO	110.0	3.590		[7]	
	88.0	3.706		[7]	
	01.7	**3.690**		[5]	
O_2	113.0	3.433		[7]	
	88.0	**3.541**		[7]	
	106.7	3.467		[5]	
Ar	**97.0**	**3.617**		[7]	
	84.0	3.689		[7]	
	93.3	3.542		[5]	

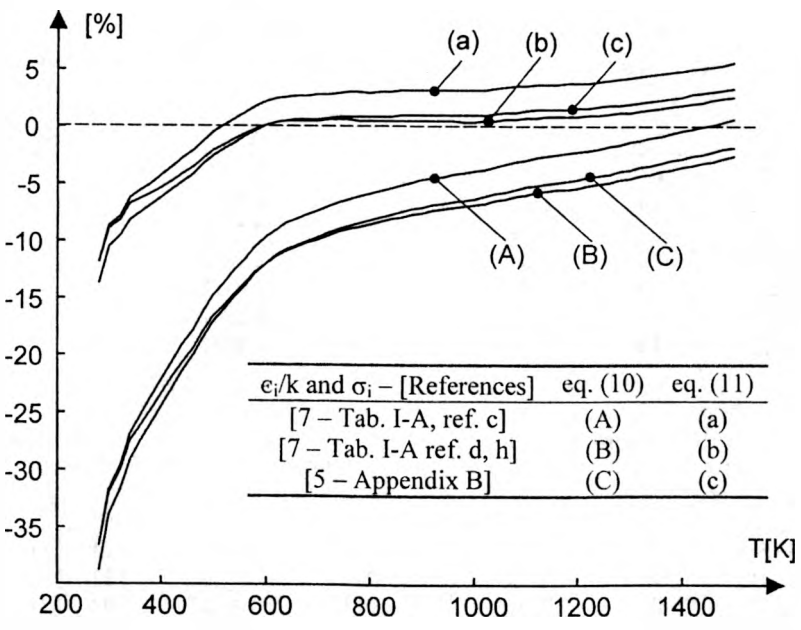

Fig. 1. Deviation of the thermal conductivity of CO_2 versus temperature T between experimental data (dashed line) and calculated from Eq. (9) for different Eucken factors according to Eqs. (10) and (11) and different parameters ε_i/k and σ_i taken from Tab. 1.

The viscosity η_i of a pure component, used in expression (8), is closely connected with the thermal conductivity [7, eq. (8.2−33)]:

$$[\lambda_i]_1 = [\eta_i]_1 \frac{15}{4} \frac{kN_A}{M_i} Eu. \tag{14}$$

So, η_i [Ns/m^2] can be calculated from

$$[\eta_i]_1 = \frac{5}{16} \sqrt{\frac{k}{\pi N_A}} \frac{\sqrt{TM_i}}{\sigma_i^2 \Omega^{(2,2)^*}(T^*)} = 8.4416 \cdot 10^{-25} \frac{\sqrt{TM_i}}{\sigma_i^2 \Omega^{(2,2)^*}(T^*)}. \tag{15}$$

According to the above considerations, the same parameters σ_i and ε_i/k bolded in Tab. 1 are used for the approximation of the viscosity.

3.2. Approximation of the experimental data of pure components

Experimental data of thermal conductivity and viscosity are usually tabulated [1]−[4]. The data from [2] were chosen for the further considerations as the most complete. To make the data more convenient for computing, the authors have introduced the approximation functions:

$$\lambda_i(T) = A_i \cdot 10^{-4} \cdot T^{B_i} + a_i \cdot 10^{-2} + b_i \cdot T \cdot 10^{-5} + c_i \cdot T^2 \cdot 10^{-8} \quad [\mathrm{W/m \cdot K}], \tag{16}$$

$$\eta_i(T) = K_i \cdot 10^{-6} \cdot T^{L_i} + k_i \cdot 10^{-5} + l_i \cdot T \cdot 10^{-8} + m_i \cdot T^2 \cdot 10^{-11} \quad [\mathrm{Ns/m^2}]. \tag{17}$$

Factors used in Equations (16) and (17) are given in Tables 2 and 3, respectively.

Table 2. Thermal conductivity approximation coefficients (Eq. (16)) for the temperature range of $T = 280:1500$. ε_{av1}, ε_{av2} — average approximation errors when the first term or full Eq. (16) is used, respectively.

i	A_i	B_i	ε_{av1}	a_i	b_i	c_i	ε_{av2}	Ref.
CO_2	0.4255	1.0631	6.5	−0.8537	2.6980	−1.5910	0.7	
N_2	2.9625	0.7830	1.1	**0.2459**	**−0.8075**	**0.4866**	**1.1**	
He	24.8795	0.7187	0.7	**0.1279**	**−0.4273**	**0.2576**	**0.7**	
Xe	0.5039	0.8349	1.2	−0.04384	0.1430	−0.08529	0.5	[2]
CO	2.6251	0.8009	0.3	−0.04679	0.1503	−0.09122	0.1	
O_2	2.5863	0.8117	1.1	**−0.07990**	**0.2602**	**−0.1564**	**1.1**	
Ar	3.1176	0.7127	1.9	−0.2486	0.8162	−0.4932	0.3	

Table 3. Viscosity approximation coefficients (Eq. (17)) for the temperature range of $T = 280:1500$. ε_{av1}, ε_{av2} — average approximation errors when the first term or full Eq. (17) is used, respectively.

i	K_i	L_i	ε_{av1}	k_i	l_i	m_i	ε_{av2}	Ref.
CO_2	0.2052	0.7589	2.7	−0.2928	0.9581	−0.5762	0.34	[2]
N_2	0.4706	0.6417	1.5	−0.1670	0.5520	−0.3348	0.37	[2]
He	0.4139	0.6777	0.2	0.02045	−0.06519	0.04033	0.02	[2]
Xe	0.2518	0.8010	2.5	−0.3915	1.2738	−0.7638	0.58	[2]
CO	0.3596	0.6877	1.0	−0.1049	0.3473	−0.2090	0.35	[2]
O_2	0.4968	0.6591	1.8	−0.2266	0.7494	−0.4533	0.64	[2]
Ar	0.4141	0.7070	1.6	−0.2095	0.6894	−0.4153	0.68	[2]

As the tables of experimental data give versus temperature with different density, so before using the approximation procedure the data were interpolated by the spline functions. In the next step the procedure of the least square method was used for the temperature step of 10 K in the range of 280–400 K and the 100 K step for the temperature range of 400–1500 K. In Tables 2 and 3 average deviations between experimental data and the Eqs. (6) and (17) are indicated. As is seen, the different average errors ε_{av1} and ε_{av2} are obtained when the first term (A_i, B_i or K_i, L_i) or full equations are used (except for of bold-faced cases in Tab. 2 where additional polynomials do not improve the approximation).

There are known approximation functions for thermal conductivity and viscosity but they differ significantly from the experimental data, especially for high temperatutes. Figure 2 shows examples of the approximation of the thermal conductivity of carbon dioxide in the range of 280–1500 K given by REID *et al.* [5], BOOTH *et al.* [10] with comparison to experimental data [2] and the approximation introduced by the authors (see Eq. (16)).

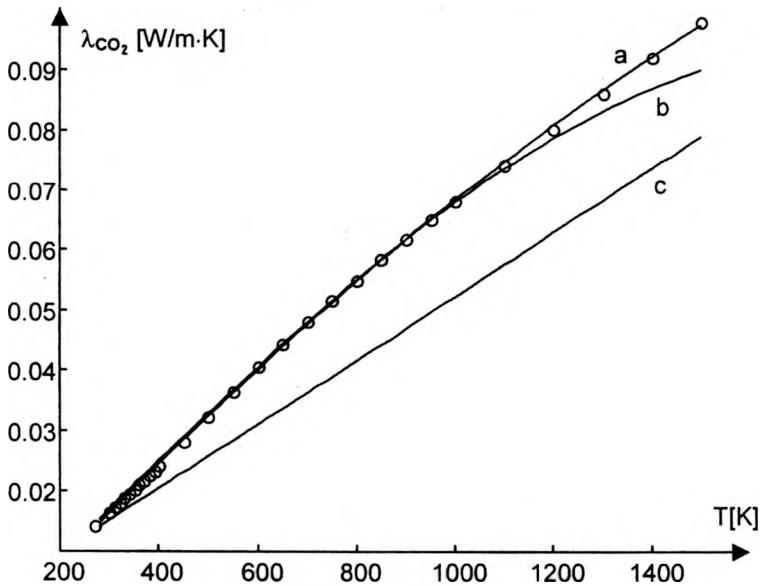

Fig. 2. Comparison of the thermal conductivity of CO_2 obtained with different approximation formulas. *a* – Eq. (16), *b* – [5], *c* – [10] (o – experimental data [2]).

4. Thermal contuctivity of gas mixtures

There are no values available of the thermal conductivity of laser gas mixtures λ_{mix}, but they can be calculated from experimental data of conductivity λ_i and viscosity η_i of components of the desired mixture according to expression (7). This possibility is indicated in Fig. 3 as λ^{I}_{mix}. In Figure 3, all possibilities of calculating of λ_{mix} are indicated as follows:

– λ^{I}_{mix} – thermal conductivity of gas mixtures based on experimental conductivity λ_i and experimental viscosity η_i,

– λ^{II}_{mix} – thermal conductivity of gas mixtures based on approximation functions of experimental conuctivity λ_i and experimental viscosity η_i,

– λ^{III}_{mix} – thermal conductivity of gas mixtures based on approximation functions of conductivity λ_i according to Eq. (9) and approximated data of viscosity η_i,

– λ^{IV}_{mix} – thermal conductivity of gas mixtures based on approximation functions of conductivity λ_i according to Eq. (9) and calculated viscosity η_i according to Eq. (15).

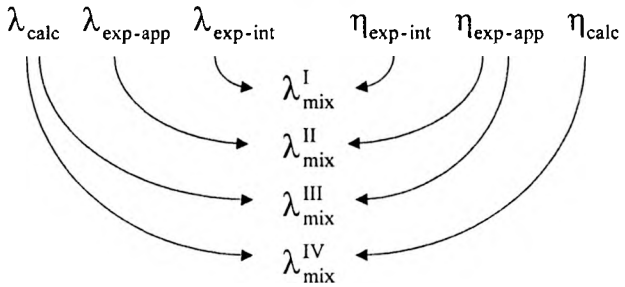

Fig. 3. Possible combinations of the calculations of the thermal conductivity of gas mixtures (calc – calculated data, exp-app – experimental data approximated with the functions (16) and (17), exp-int – experimental data interpolated with the spline functions.

The thermal conductivities λ^{II}_{mix}, λ^{III}_{mix} and λ^{IV}_{mix} are convenient for practical use, but different accuracy is obtained. Figure 4 shows thermal conductivities λ^{II}_{mix}, λ^{III}_{mix} and λ^{IV}_{mix} and λ^{I}_{mix}. The characteristics were plotted for $CO_2:N_2:He:Xe = 0.19:0.19:0.57:0.05$ mixture as an example. As can be seen, λ^{II}_{mix} is the closest to the experimental data, and this method (see Fig. 3) of obtaining thermal conductivity of any laser gas mixture is used below.

For further considerations thermal conductivity of the desired mixture is calculated using approximation formula

$$\lambda_{mix} = M_i \cdot 10^{-4} \cdot T^{N_i} \quad [W/m \cdot K]. \tag{18}$$

Coefficients M_i and N_i for some typical gas laser mixtures are listed in Tab. 4. It was recognised that the average error of approximation given by Eq. (18) is less than 1.3% for all data in Tab. 4, which is satisfactory in comparison with the initial data of λ_i and η_i approximated in Tabs. 2 and 3. Thus, an additional polynomial, as in Eq. (16) or (17), can be omitted.

Thermal conductivity of all mixtures given in Tab. 4 is plotted in Fig. 5. As is seen, the CO laser mixtures have the highest and Xe laser mixtures the lowest thermal conductivity, which is due to contents of helium in the mixture. The influence of Xenon is visible in CO_2 laser mixture characteristics. It decreases the thermal conductivity (the test composition without Xenon is given in the figure for comparison).

T a b l e 4. Thermal conductivity of typical laser gas mixtures for three chosen kinds of lasers. The compositions of mixtures are from the references indicate. Thermal conductivity can be approximated by: $\lambda_{mix} = M_i \cdot 10^{-4} \cdot T^{N_i}$ [/m·K] with an average error less than 1.3 %.

Composition:	i	CO_2	N_2	He	Xe	CO	O_2	Ar	Refs.	M_i	N_i
CO_2 laser	(1)	0.1900	0.1900	0.5700	0.0500	–	–	–	[11, 12]	6.4983	0.7908
	(2)	0.2000	0.2000	0.6000	–	–	–	–	[13]	7.3717	0.7855
	(3)	0.1357	0.1357	0.6786	0.0500	–	–	–	[14, 15]	8.7987	0.7733
CO laser	(4)	–	0.1800	0.7591	0.0352	0.0253	0.0004	–	[16]	14.3223	0.7287
	(5)	–	0.1600	0.7860	–	0.0500	0.0040	–	[17]	16.2950	0.7216
	(6)	–	–	0.8738	0.0349	0.0874	0.0039	–	[18]	17.1784	0.7327
	(7)	–	–	0.9918	0.0265	0.0882	0.0035	–	[19]	17.8266	0.7307
Xe laser	(8)	–	–	0.2000	0.0100	–	–	0.7900	[20]	4.8796	0.7237
	(9)	–	–	0.4000	0.0100	–	–	0.5900	[21, 22]	7.3224	0.7273
	(10)	–	–	0.3990	0.0025	–	–	0.5985	[23]	7.4126	0.7261
	(11)	–	–	0.4900	0.0100	–	–	0.5000	[20]	8.7085	0.7279
	(12)	–	–	0.5985	0.0025	–	–	0.3990	[21]	10.8742	0.7266

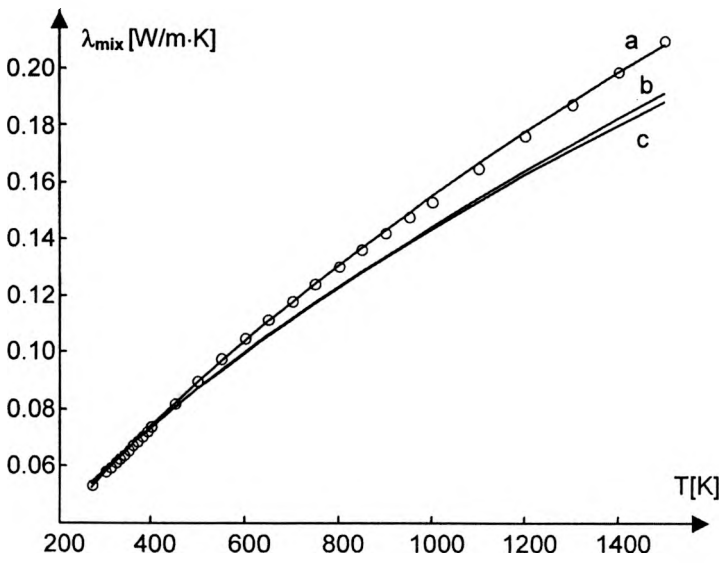

Fig. 4. Thermal conductivity of the CO_2 laser mixture ($CO_2 : N_2 : He : Xe = 1:1:3+5\%$ Xe) obtained with different methods of calculations: o — λ_{mix}^{I}, *a* — λ_{mix}^{II}, *b* — λ_{mix}^{III}, *c* — λ_{mix}^{IV}.

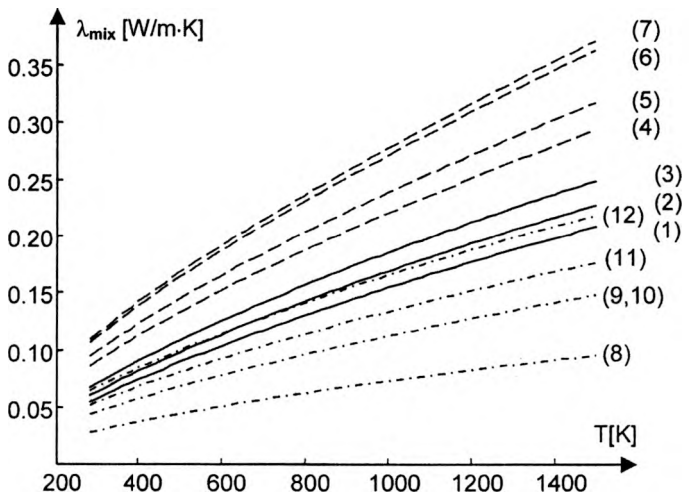

Fig. 5. Thermal conductivity of chosen laser mixtures given in Tab. 4. Indexes of plots are adequate to index *i* in the table (dotted lines — Xe lasers, dash-dotted lines — CO lasers, solid lines — CO_2 lasers).

5. Temperature distribution in slab-waveguide gas laser

Temperature distribution in slab-waveguide gas lasers can be calculated from the well-known heat transfer elliptic-type equation

$$\operatorname{div}(\lambda_i(T)\operatorname{grad}(T)) = -Q_i \tag{19}$$

where: $\lambda_i(T)$ – thermal conductivity of the gas mixture, Q_i – input power per unit volume [W/m^3].

The solution of the equation has been obtained with some additional assumptions:

– constant temperature of the laser walls $\mathbf{T}_w$ (Dirichlet type boundary conditions),

– the length l of the waveguide is much greater than transverse dimensions x, y ($\partial/\partial z \approx 0$) – see Fig. 6,

– the input power is uniformly distributed in the volume of the laser cavity, (Q is constant for $|x| < w$, $|y| < D$, and zero otherwise) – see Fig. 6,

– thermal conductivity depends on temperature.

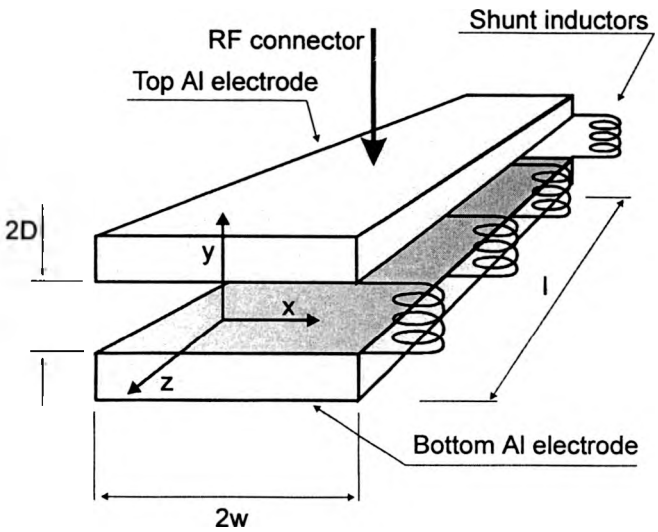

Fig. 6. Geometry of the slab-waveguide structure formed by two Al electrodes. Transverse dimensions 2D and 2w and length l of the slab are given. Shunt inductors (used for equalising the RF voltage distribution) are indicated as well.

Temperature distributions were analysed in the literature for a conventional electric-discharge tube laser [23] and RF excited waveguide structure [24]. Considerations in the papers cited were limited to the maximum temperature of 700 K, and specific laser mixtures.

Nowadays high power gas lasers are constructed as slabs, they use different media (CO_2, CO, Xe) with various compositions [12]–[22]. A uniform distribution of the input power is achieved by a transverse RF excitation. A high mode volume in slab lasers is usually obtained using an unstable configuration of the optical resonator. The best quality of the output laser beam is reached in an open structure of the laser cavity, that is, in a slab-waveguide without sidewalls. In that way, a hybrid structure of the laser is obtained: waveguiding propagation between electrodes, and free space propagation in the lateral direction (see Fig. 6).

Examples of the temperature distribution in the slab-waveguide lasers of the transverse dimensions $2w = 40$ mm, $2D = 2$ mm (see Fig. 6) have been calculated using the finite element method. The characteristics are calculated for chosen lasers from Tab. 4 with additional data given in Tab. 5 (see Fig. 7). The appropriate specific power and a wall temperature were matched to the chosen kind of the laser (CO_2 laser, CO laser, and Xe laser) according to the literature cited. Two cross-sections (in the lateral direction x and the waveguiding direction y) are shown in the figure. As is shown, the distribution is perfectly uniform along x-axis. Maximum and average temperatures (Tab. 5) are quite high for Xe lasers as a consequence of

Table 5. Maximum T_{max} and average T_{av} temperatures of gas mixtures obtained in chosen lasers for specific power Q and wall temperature T_w (indices i are adequate to the indexes in Tab. 4).

Laser	i	Q_i [W/cm^3]	T_w [K]	[Ref.]	T_{max} [K]	T_{av} [K]
CO_2	(1)	52	288	[12]	609	495
	(2)				586	480
	(3)				563	465
CO	(6)	69	2453	[17]	505	412
Xe	(10)	120	288	[22]	1024	772
	(12)				844	785

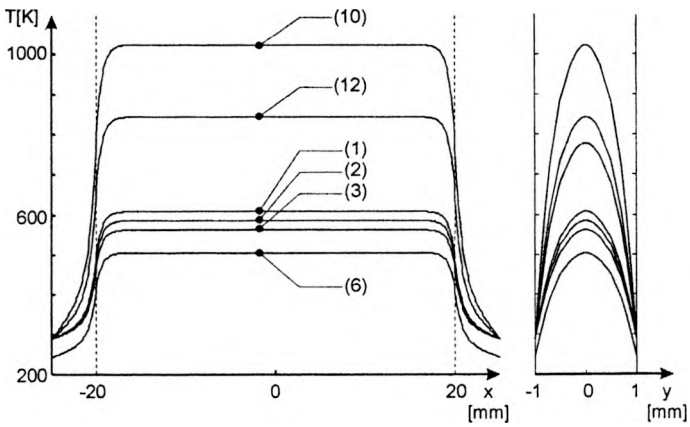

Fig. 7. Temperature profiles in chosen slab-waveguide lasers in x- and y-directions. (1), (2), (3) – CO_2 lasers, (6) – CO laser, (10), (12) – Xe laser (see Tab. 4).

relatively high specific power and low thermal conductivity (Tab. 4 and Fig. 5). Low temperatures for CO lasers are obtained because of strong cooling with methanol ($T_w = -30$ °C [17]) and high thermal conductivity (Tab. 4 and Fig. 5).

Figure 8 shows the full temperature distribution in the Xe slab-waveguide laser ($i = 10$, Tabs. 4 and 5) as an example. As can be seen, the temperature drops fast outside the laser cavity. It was found that the dimensions r_w and r_D of the laser reservoir affect the temperature inside the laser cavity very weakly if only $r_w = r_D > 4D$.

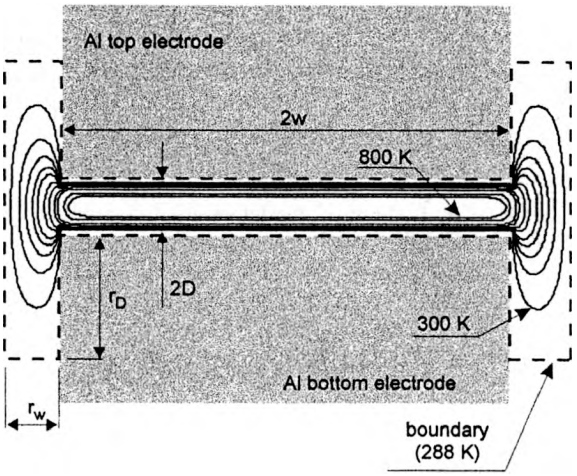

Fig. 8. Transverse distribution of temperature in a slab-waveguide with cross-section: $2D = 2$ mm and $2w = 40$ mm. The boundaries of integration area are indicated ($r_w = r_D = 5$ mm). Isotherms are plotted every 50 K.

6. Conclusions

Approximation functions for the experimental data of thermal conductivity and viscosity of chosen gases CO_2, N_2, He, Xe, CO, O_2, and Ar are given in the paper. The chosen gases are the components of the most popular high power gas lasers, like CO_2, CO or Xe lasers. The functions give the possibility of calculating the thermal conductivity of arbitrarily chosen laser gas mixtures versus temperature inside the laser cavity. Calculations of the temperature distribution inside the cavities of modern, transversely RF excited gas lasers in waveguide or slab-waveguide structurs are possible as well.

Different methods of prediction of thermal conductivity and viscosity versus temperature of gases have been compared. Finally, the experimental data of thermal conductivity and viscosity of pure components have been applied in the paper, as being the most reliable.

The approximation functions introduced in the paper are based on the carefully chosen experimental data, and they cover a wide range of temperatures from 280 to 1500 K. The functions elaborated give the possibility of proper designing the gas laser devices, especially high power ones, where estimation of the temperature conditions inside the laser cavities plays an important role.

Examples of the thermal conductivity for typical CO_2, CO and Xe laser gas media versus temperature are given and compared. Temperature distributions for the afore mentioned three RF excited laser media in the same slab-waveguide structure are given as an example of approximation formulas introduced. The full algorithm for predicting the thermal conductivity of a laser gas mixture can be reduced to formulas (7), (8), (16), and (17) and Tabs. 2 and 3.

As is known, the temperature of the laser mixture can influence the quality of the laser beam due to gain cross-section of the laser cavity, and it can change the spectral peoperties of the laser radiation. So, knowledge of the temperature distribution in the laser cavity can be used for prediction of the general optical properties of the laser.

Acknowledgments — The authors wish to thank Krzysztof Abramski for informative discussions and Ignac Sulikowski for his expert technical assistance. The work was partly supported by the State Committee for Scientific Research (KBN), Poland, Grant No. 8 T11B 02118.

References

[1] *CRC Handbook of Chemistry and Physics*, 77th edition, [Ed.] D. R. Lide, CRC Press Inc., London, Tokyo 1996.
[2] VARGAFTIK N. B., *Handbook of Physical Properties of Liquids and Gases: Pure Substances and Mixtures*, Hemisphere Publ. Corporation, Springer-Verlag, Washington, Paris, London, 2nd ed., 1975.
[3] HILSENBRATH J., *et al., Tables of Thermodynamic and Transport Properties of Aair, Argon, Carbon Dioxide, Carbon Monoxide, Hydrogen, Nitrogen, Oxygen, and Steam*, Pergamon Press, Oxford, London, New York, Paris 1960.
[4] RABINOVICH V. A., VASSERMAN A. A., NEDOSTUP V. I., VEKSLER L. S., *Thermophysical Properties of Neon, Argon, Krypton, and Xenon*" [Ed.] Th. B. Selover, Jr., Hemisphere Publishing Corporation, Springer-Verlag, New York, London 1988.
[5] REID R. C., PRAUSNITZ J. M., POLING B. E., *The Properties of Gases and Liquids*, McGraw-Hill Book Company, New York, London, Paris, Tokyo 1987.
[6] NEUFELD P. D., JANZEN A. R., AZIZ R. A., J. Chem. Phys. **57** (1972), 1100.
[7] HIRSCHFELDER J. O., CURTISS CH. F., BIRD R. B., *Molecular Theory of Gases and Liquids*, John Wiley and Hall, Ltd., London 1954.
[8] MASON E. A., SAXENA S. C., The Physics of Fluids **1** (1958), 361.
[9] SAAD M. A., *Thermodynamics, Principle and Practice*, Prentice-Hall International, Ltd., London 1997.
[10] BOOTH D. J., GIBBS W. E. K., Report 413, Defence Standards Laboratories, Maribyrong, Victoria, Australia, Nov. 1970.
[11] HE D., HALL D. R., Appl. Phys. Lett. **43** (1983), 726.
[12] JACKSON P. E., BAKER H. J., HALL D. R., Appl. Phys. Lett. **54** (1989), 1950.
[13] HEEMAN-ILIEVA M. B., UDALOV YU. B., WITTEMAN W. J., PETERS P. J., HOEN K., OCHKIN V. N., J. Appl. Phys. **74** (1993), 4786.
[14] HEEMAN-ILIEVA M. B., UDALOV YU. B., HOEN K., WITTEMAN W. J., Appl. Phys. Lett. **64** (1994), 673.
[15] PEARSON G. N., HALL D. R., IEEE J. Quant. Electron. **25**, (1989), 245.
[16] KANAZAWA H., MATSUZAKA F., UEHARA M., KASUYA K., IEEE J. Quant. Electron. **30** 1994), 1448.
[17] COLLEY A. D., VILLARREAL F., BAKER H. J., HALL D. R., Appl. Phys. Lett. **64** (1994), 2916.
[18] ZHAO H., BAKER H. J., HALL D. R., Appl. Phys. Lett. **59** (1991), 1281.
[19] TSKHAI S. N., UDALOV YU. B., PETERS P. J. M., WITTEMAN W. J., Appl. Phys. Lett. **66** (1995), 801.
[20] MORELY R. J., WENDLAND J. J., BAKER H. J., HALL D. R., Opt. Commun. **142** (1997), 244.
[21] UDALOV Y. B., PETERS P. J., HEEMAN-ILIEVA M. B., ERNST F. H. J., OCHKIN V. N., Appl. Phys. Lett. **63** (1993), 721.
[22] VITRUK P. P., MORLEY R. J., BAKER H. J., HALL D. R., Appl. Phys. Lett. **67** (1995), 1366.
[23] LADERMAN A. J., BYRON S. R., Appl. Phys. Lett. **42** (1971), 3138.
[24] PARAZZOLI C. G., KUEI-RU CHEI, IEEE J. Quant. Electron. **22** (1986), 479.

Received July 16, 2000